

Analytical Model for Capillary Evaporation Limitation in Thin Porous Layers

Y. X. Wang* and G. P. Peterson†

Rensselaer Polytechnic Institute, Troy, New York 12180

Fluid flow and heat transfer in thin porous layers are of fundamental importance in numerous applications, including the development of high power-density electronics cooling devices, loop heat pipes, aerospace radiators, as well as micro fuel cells. A two-dimensional analytical model has been developed to evaluate the pressure distribution and capillary evaporation limitation in a uniformly heated thin porous layer and the effects of the porous structure and properties of the working fluid on the capillary evaporation process. Two types of porous materials, sintered powder and layers of screen mesh, with different characteristics were investigated. The results indicated that the maximum capillary evaporation heat transfer is proportional to the thickness and the permeability of the thin porous layer, but that increasing the thickness of the porous layer can result in higher superheat. Higher Bond numbers were shown to correspond to higher capillary evaporation heat-transfer limitations. By comparison, the sintered wick structure had a significantly higher effective conductivity and a higher capillary pumping pressure than the mesh screen. As a result, the maximum evaporation heat-transfer rate for the sintered powder layer was much higher than for any of the mesh screen layers evaluated.

Nomenclature

a_l	= length of studied porous layer, m
Bo	= Bond number
b_l	= width of studied porous layer, m
C_m	= constant
d_p	= diameter of particles, m
g	= gravity acceleration, m/s^2
g_0	= source term, $g_0 = -v_l q'' / K \delta h_{fg}$, N/m^4
h_{fg}	= latent heat of vaporization, J/kg
K	= permeability, m^{-2}
k_{eff}	= effective thermal conductivity, $W/m K$
P	= pressure, Pa
P_{cap}	= capillary pressure, Pa
P_{sat}	= saturated pressure, Pa
P^*	= pressure drop, $P^* = P(x, y) - P_{sat}(T_{sat})$, Pa
q''	= heat flux per unit area, W/m^2
q''_{max}	= maximum evaporation heat flux, W/m^2
Re	= Reynolds number
$r_{cap,e}$	= radius of liquid meniscus, m
T_i	= liquid–vapor interfacial temperature, K
T_s	= surface temperature of the solid wall, K
T_{sat}	= saturated temperature of the liquid, K
u_D	= Darcy velocity in x direction, m/s
v_D	= Darcy velocity in y direction, m/s
α	= contact angle, grade
γ_l	= dynamic viscosity of the working fluid, m^2/s
δ	= thickness of the porous layer, m
ε	= porosity
μ_l	= viscosity of the working fluid, $N \cdot s/m^2$
ρ_l	= liquid density, kg/m^3
σ	= surface tension, N/m

Subscripts

cap	= capillary
e	= evaporator
l	= liquid phase
max	= maximum

Introduction

PHASE-CHANGE heat transfer and fluid flow in thin porous layers have a fundamental importance in a wide variety of applications in the electronics cooling, nuclear, chemical, and biochemical industries. This is especially true in the microelectronic industry, where increases in the number of integrated circuits on a single chip and the operating speed are both increasing, resulting in significant increases in the power density. This ever-increasing power density has forced the industry to develop more advanced cooling devices in order to accommodate what in the very near future will reach or exceed $200 W/cm^2$ in a single chip, which conventional cooling techniques cannot effectively dissipate. Alternative cooling methods, such as liquid impingement, capillary pumped loop systems, and flat heat-pipe heat spreaders, have not proven to be capable of rejecting the required level of heat in most applications. In flat heat pipes, loop heat pipes, and other phase-change cooling devices the porous media used to return the liquid from the condenser section to the evaporator are typically the limiting factors. These porous wick structures are usually fabricated from sintered powder, metal screen, metal foam, or other highly conductive porous media.

The maximum heat-transport capacity on the surface of these porous media is determined by a combination of the interfacial area, the frictional pressure, and the capillary pumping capacity of the porous structure. In addition to the capillary limitation, the boiling limitation often becomes important in applications with extremely high heat fluxes. Because the wick structure, porosity, thickness, and size of the conduit all have a significant effect on the evaporation process and the capillary action, it is necessary to evaluate these effects simultaneously.

In addition to the transport of the working fluid by the capillary pumping pressure, the porous structure has a significant effect on the heat and mass transport processes. Although previous investigators^{1–3} have shown that the evaporation heat transfer from a porous surface is directly related to the capillary flow, effective thermal conductivity, and permeability, the exact nature of this relationship is not well understood. Clearly the evaporation process in fine porous media is fundamentally different from pool boiling,

Received 7 May 2002; revision received 16 October 2002; accepted for publication 18 November 2002. Copyright © 2002 by the American Institute of Aeronautics and Astronautics, Inc. All rights reserved. Copies of this paper may be made for personal or internal use, on condition that the copier pay the \$10.00 per-copy fee to the Copyright Clearance Center, Inc., 222 Rosewood Drive, Danvers, MA 01923; include the code 0887-8722/03 \$10.00 in correspondence with the CCC.

*Research Assistant Professor of Mechanical Engineering, Department of Mechanical, Aerospace and Nuclear Engineering, Member AIAA.

†Professor of Mechanical Engineering, Office of the Provost, Room 3018, Troy Building, Fellow AIAA.

but the mode and the precise point at which this difference begins to become important is not well understood. When the diameter of the particle or the wire becomes small, that is, when the Bond number $Bo \leq 0.01$, the surface temperature increases monotonically with the heat flux.⁴ In addition, the formation of vapor film occurs at the critical heat flux, which was proportional to the permeability of the porous layer. Experiments conducted by Sondergeld and Turcotte² demonstrated that no significant superheat is required to initiate the surface evaporation of the thin liquid film.

The objective of the present investigation focuses on developing an analytical model to predict the heat-transfer performance of the thin porous layer and the capillary evaporation limitation in thin porous media structures. The effects of thickness, porosity, and permeability of the porous layer on the maximum heat-transport capacity and temperature difference/superheat have been investigated and evaluated.

Mathematical Model

In many heat-transfer applications a thin homogeneous porous layer is bonded onto a uniformly heated, solid surface, as illustrated in Fig. 1. The heat-transfer process typically occurs at a horizontal impermeable bounding surface and the fluid flow is driven by the capillary force created by the liquid curvature. Evaporation is assumed to take place at the surface of the porous layer at which the liquid vapor interface is formed. In this process uniform heat flux is added to the solid surface, and the working fluid evaporates from the surface of the porous media. The fluid flow typically occurs from the outer edges towards the center of the heated area and is driven by the capillary force created caused by the variation of the curvature of the liquid surface between the center region and the outer edges.

The porous structure can be made of sintered powder, metal screen, metal foam, or other porous media. The maximum capillary evaporation heat-transport capacity of the porous layer is reached when the frictional pressure drop through the layer is equal to or less than the capillary pumping capacity of the wick structure. In addition to the capillary limitation, the boiling limitation might also become relevant, particularly in very fine, thin porous layers. The heat transfer and fluid flow are governed by mass, energy, and momentum conservation, and because the liquid movement in the direction perpendicular to the surface is much smaller than that occurring in a direction parallel to the surface it can be treated as two-dimensional flow in the thin layer.

Mass Conservation

Because the evaporation only takes place in the porous surface and the thickness of the porous capillary layer is much smaller

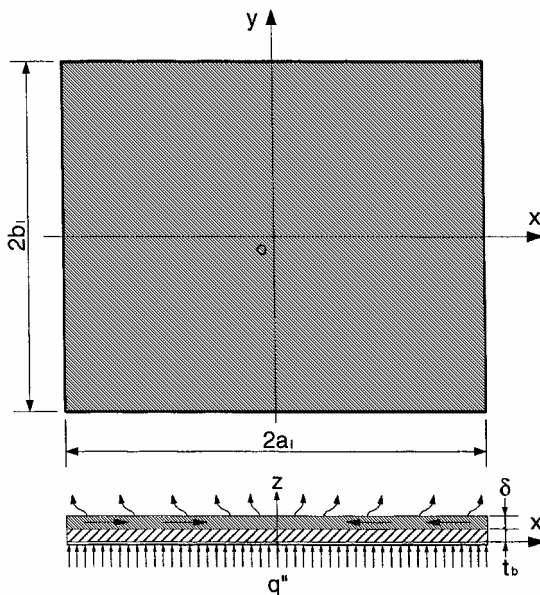


Fig. 1 Evaporation in a heated thin porous layer.

compared to the width and length of the layer, the control volume in the z direction can be considered as unity. The conservation of mass through the porous media can be expressed as

$$\frac{\partial u_D}{\partial x} + \frac{\partial v_D}{\partial y} + \frac{q''}{\delta \rho_l h_{fg}} = 0 \quad (1)$$

Momentum Equation

At low velocities and low Reynolds numbers, and neglecting the viscous effects, the momentum equation for flow in the porous media can be characterized by Darcy's law as

$$u_D = -\frac{K}{\mu_l} \frac{\partial P}{\partial x} \quad (2)$$

$$v_D = -\frac{K}{\mu_l} \frac{\partial P}{\partial y} \quad (3)$$

As the saturated working fluid fills the porous material in the entire heated area (fluid-saturated porous media), the pressure around the boundary is equal to the saturation pressure. The boundary conditions for the problem described here can be defined as

$$x = 0, \quad \left. \frac{\partial P}{\partial x} \right|_{x=0} = 0 \quad (4a)$$

$$y = 0, \quad \left. \frac{\partial P}{\partial y} \right|_{y=0} = 0 \quad (4b)$$

$$x = a_l, \quad P(x, y) = P_{\text{sat}}(T_{\text{sat}}) \quad (4c)$$

$$y = b_l, \quad P(x, y) = P_{\text{sat}}(T_{\text{sat}}) \quad (4d)$$

Substituting Eqs. (2) and (3) into Eq. (1) yields

$$\frac{\partial^2 P}{\partial x^2} + \frac{\partial^2 P}{\partial y^2} - \frac{\nu_l q''}{K \delta h_{fg}} = 0 \quad (5)$$

Assuming $P^* = P(x, y) - P_{\text{sat}}(T_{\text{sat}})$ and $g_0 = -\nu_l q'' / K \delta h_{fg}$, Eq. (5) and the associated boundary conditions become

$$\frac{\partial^2 P^*}{\partial x^2} + \frac{\partial^2 P^*}{\partial y^2} + g_0 = 0 \quad (6)$$

$$x = 0, \quad \left. \frac{\partial P^*}{\partial x} \right|_{x=0} = 0 \quad (7a)$$

$$y = 0, \quad \left. \frac{\partial P^*}{\partial y} \right|_{y=0} = 0 \quad (7b)$$

$$x = a_l, \quad P^*(x, y) = 0 \quad (7c)$$

$$y = b_l, \quad P^*(x, y) = 0 \quad (7d)$$

To solve the differential equation shown in Eq. (6), a transformation is made to obtain a homogeneous equation and the relevant boundary conditions. If

$$P^* = \hat{P} - (g_0/2)x^2 + (g_0/2)a_l^2 \quad (8)$$

the differential equation and the boundary conditions become

$$\frac{\partial^2 \hat{P}}{\partial x^2} + \frac{\partial^2 \hat{P}}{\partial y^2} = 0 \quad (9)$$

$$x = 0, \quad \left. \frac{\partial \hat{P}}{\partial x} \right|_{x=0} = 0 \quad (10a)$$

$$x = a_l, \quad \hat{P}(x, y) = 0 \quad (10b)$$

$$y = 0, \quad \left. \frac{\partial \hat{P}}{\partial y} \right|_{y=0} = 0 \quad (10c)$$

$$y = b_l, \quad \hat{P}(x, y) = \frac{g_0}{2}(x^2 - a_l^2) \quad (10d)$$

The general solution for Eq. (9) with the corresponding boundary conditions as presented in Eq. (10) can then be determined as

$$\hat{P}(x, y) = \sum_{m=1}^{\infty} c_m \cosh(\beta_m y) \cos(\beta_m x) \quad (11)$$

where β_m is the positive root of

$$\cos(\beta_m a_l) = 0 \quad (12)$$

and

$$\beta_m = \frac{(2m-1)\pi}{2a_l}, \quad m = 1, 2, 3, \dots \quad (13)$$

The coefficient c_m should be determined such that this solution also satisfies the nonhomogenous boundary condition. Application of the nonhomogenous boundary condition at $y = b_l$ yields

$$\frac{g_0}{2}(x^2 - a_l^2) = \sum_{m=1}^{\infty} c_m \cosh(\beta_m b_l) \cos(\beta_m x) \quad (14)$$

where c_m can be defined as

$$c_m = \frac{g_0}{a_l \cosh(\beta_m b_l)} \int_0^{a_l} \cos(\beta_m x) (x^2 - a_l^2) dx \quad (15)$$

Integrating Eq. (15) yields

$$c_m = -\frac{g_0}{a_l \cosh(\beta_m b_l)} \frac{2}{\beta_m^3} \sin(\beta_m a_l) \quad (16)$$

The resulting solution for the two-dimensional pressure distribution is

$$\hat{P}(x, y) = -\frac{2g_0}{a_l} \sum_{m=1}^{\infty} \frac{\sin(\beta_m a_l)}{\beta_m^3 \cosh(\beta_m b_l)} \cosh(\beta_m y) \cos(\beta_m x) \quad (17)$$

or

$$P(x, y) = P_{\text{sat}}(T_{\text{sat}}) - \frac{2g_0}{a_l} \sum_{m=1}^{\infty} \frac{\sin(\beta_m a_l)}{\beta_m^3 \cosh(\beta_m b_l)} \cosh(\beta_m y) \cos(\beta_m x) - \frac{g_0}{2}(x^2 - a_l^2) \quad (18)$$

Capillary Limitation

The pressure difference required to return the liquid from the condenser section to the evaporator section is generated by the capillary force at the liquid–vapor interface on the surface of the porous media, which is directly related to the meniscus radii of the interface by the Laplace–Young equation. This pressure difference can be expressed as

$$\Delta P_{\text{cap}} = 2\sigma (\cos \alpha / r_{\text{cap,e1}} - \cos \alpha / r_{\text{cap,e2}}) \quad (19)$$

where $r_{\text{cap,e1}}$ and $r_{\text{cap,e2}}$ are the radii of liquid meniscus formed in the porous cells at the center and the boundaries of the capillary layer, respectively. The minimum radius of the liquid meniscus $r_{\text{cap,e1}}$ could be estimated for special capillary structures as addressed by Peterson.⁵ The radius of liquid meniscus on the boundary $r_{\text{cap,e2}}$ is much larger than the meniscus radius in the center area so that the last term in Eq. (19) can be neglected.

Continuous transport of liquid to the interfacial evaporation area requires that the friction pressure drop caused by fluid flow be less than the capillary pressure produced by Eq. (19), that is

$$\Delta P_{\text{cap}} \geq \Delta P_l \quad (20)$$

The total liquid pressure drop from the outer edge to the center of the porous layer can be determined by Eq. (18) as

$$\Delta P_l = P_{\text{sat}}(T_{\text{sat}}) - P(0, 0) \quad (21)$$

$$\Delta P_l = \frac{2g_0}{a_l} \sum_{m=1}^{\infty} \frac{\sin(\beta_m a_l)}{\beta_m^3 \cosh(\beta_m b_l)} - \frac{g_0}{2} a_l^2 \quad (22)$$

When the capillary pressure is equal to the liquid viscous pressure drop, the heat flux reaches a maximum value, and dryout occurs. The maximum capillary evaporation heat flux is obtained by coupling Eqs. (19) and (22) or

$$q''_{\text{max}} = \frac{2K \delta h_{\text{fg}} \sigma \cos \alpha}{\gamma_l} \left(\frac{1}{r_{\text{cap,e1}}} - \frac{1}{r_{\text{cap,e2}}} \right) \times \left[\frac{a_l^2}{2} - \frac{2}{a_l} \sum_{m=1}^{\infty} \frac{\sin(\beta_m a_l)}{\beta_m^3 \cosh(\beta_m b_l)} \right]^{-1} \quad (23)$$

It is clear from the preceding relationship that the critical capillary evaporation heat transfer in the thin porous layer is proportional to the permeability and the thickness of the porous layer. However, the larger permeability results in a smaller capillary pumping capacity as a result of a reduction in the curvature of the meniscus.

Results and Discussion

As mentioned earlier, the capillary evaporation heat-transfer performance of the thin porous layer can be evaluated by the analytical expression given in Eq. (23). Sintered powders and mesh screen layers are studied here as typical examples of the types of porous materials used in many heat-transfer applications. The results indicated that the fundamental parameters of the porous media such as the pore size, porosity, permeability, and effective thermal conductivity all have a significant effect on the maximum heat-transport capacity of the evaporation processes.

Pressure Distribution

Working fluid flows to the evaporator area, driven by the capillary force, and this flow results in a pressure drop in the liquid. The two-dimensional pressure distribution in the porous layer for different configurations can be obtained by Eq. (18). The pressure distribution in the porous layer is primarily affected by the geometric parameters of the porous layer, the heat flux, and the characteristics of the porous structure such as permeability and porosity. The pressure distribution for an example case with $a_l = b_l = 40$ mm, $\delta = 1.0$ mm, and heat flux $q'' = 1.3 \times 10^5$ W/m² is presented in Fig. 2. The porous layer is assumed to be sintered copper powder with $\varepsilon = 0.52$ and $K = 9.0 \times 10^{-13}$. Water is assumed to be the working fluid. The pressure illustrated in Fig. 2 is the dimensionless pressure defined as $P(x, y)/P_{\text{sat}}$. Because of the larger flow area and hence smaller flow rate in the outer area, the pressure drop in this region is smaller than in the center region.

Capillary Evaporation Limitation

As indicated earlier, the maximum capillary evaporation heat flux in the thin porous layer can be evaluated by Eq. (23). It is obvious that the evaporation heat-transfer performance of the porous layer is affected by the fundamental parameters of porous structure such as permeability, porosity, pore size, thickness, and effective thermal conductivity of the layer as well as the thermophysical properties of the working fluid. The operating temperature of the working fluid determines these properties and therefore affects the evaporation heat-transfer performance.

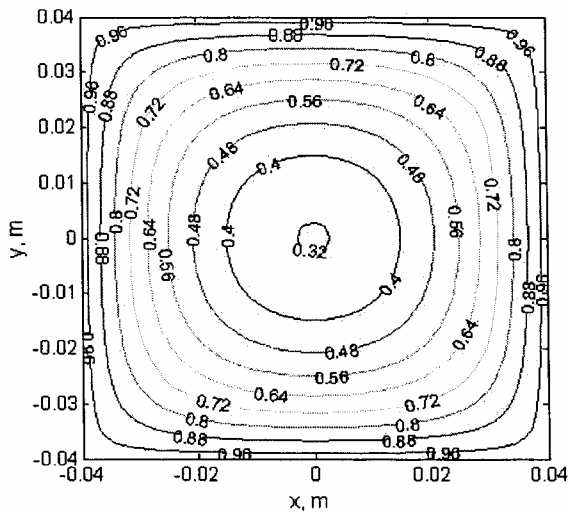


Fig. 2 Pressure distribution in the porous layer with $a_1 = b_1 = 40$ mm and $q'' = 1.3 \times 10^5$ W/m².

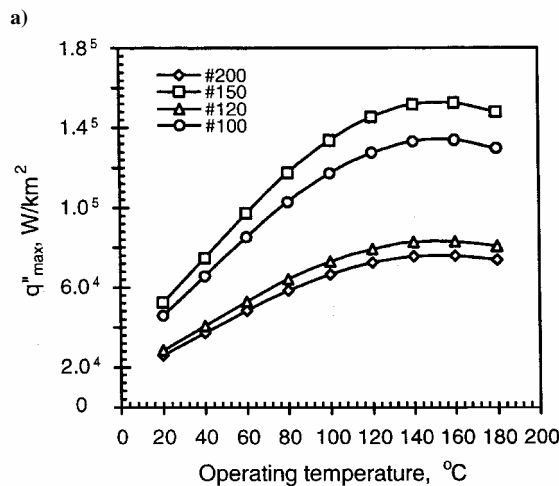
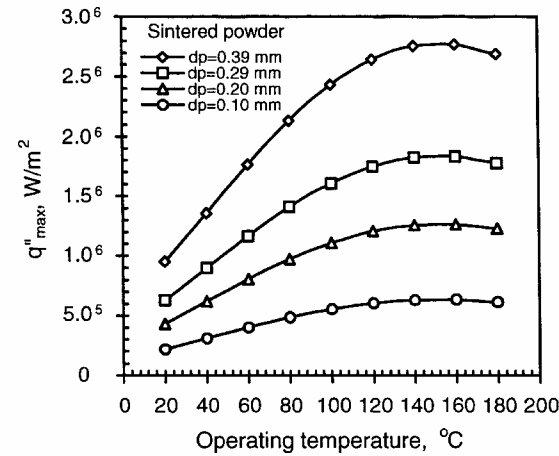


Fig. 3 Effect of the operating temperature on evaporation heat transfer for a) sintered powder and b) mesh screen.

The maximum capillary evaporation heat flux is presented in Figs. 3a and 3b for sintered copper powder and mesh screen, respectively. It is apparent that the maximum evaporation heat flux increases with increases in the operating temperature until the operating temperature reaches a value of 150°C (for water), at which time it begins to decrease. This implies that the optimum operating temperature range for water is 20–150°C.

The predicted capillary evaporation heat transfer for the sintered copper powder layer is much higher than for the copper mesh screen,

as shown in Fig. 3. The porous layer with a larger particle size has a larger capillary evaporation heat-transfer flux. For mesh screens the maximum evaporation heat flux for #150 mesh is larger than #120, and the capillary performance of the #150 is very close to that obtained for #100 mesh. This implies that #150 and #100 would both be good wick structure candidates.

As mentioned earlier, the characteristics of the porous layer structure have a significant effect on the capillary evaporation heat transfer. The characteristics of the porous layer can be described by the Bond number, which is defined as

$$Bo = \frac{g(\rho_l - \rho_v)K}{\sigma \varepsilon} \quad (24)$$

For the porous media with fine particles, the Bond number is small, and the maximum capillary evaporation heat flux of the thin porous layer increases rapidly by increasing with an increasing Bond number as shown in Fig. 4. Larger permeability and smaller porosity also enhance the capillary evaporation level.

Increasing the thickness of the porous layer can decrease the liquid flow velocity in the layer, therefore decreasing the frictional pressure drop. As indicated in Eq. (23), the maximum evaporation heat transfer is proportional to the thickness of the porous layer. However, thicker porous layers result in greater superheats, as illustrated in Fig. 5. As previous investigations have indicated, the evaporation takes place on the surface of the liquid film,^{3,4,6} and the heat transfer through the porous layer is mainly by conduction. The temperature difference (superheat) through the layer can be estimated by the one-dimensional heat-conduction equation

$$\Delta T_s = T_s - T_i = q'' \delta / k_{\text{eff}} \quad (25)$$

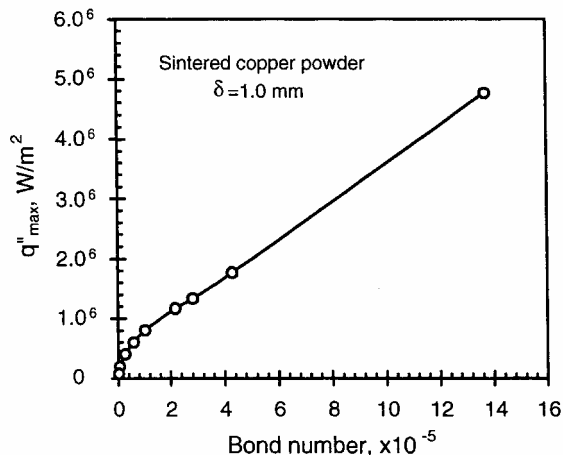


Fig. 4 Effect of the bond number on the evaporation heat transfer.

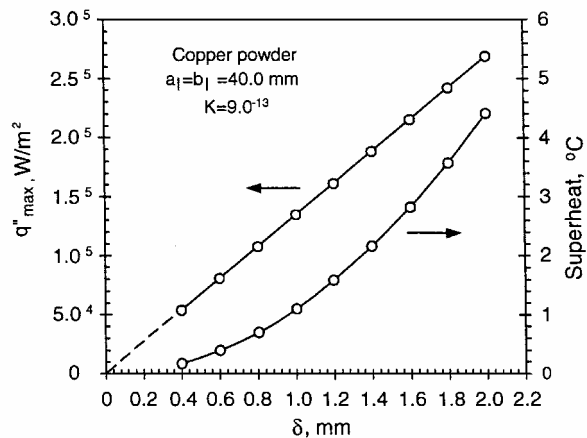


Fig. 5 Effect of the thickness of the layer on the evaporation heat transfer.

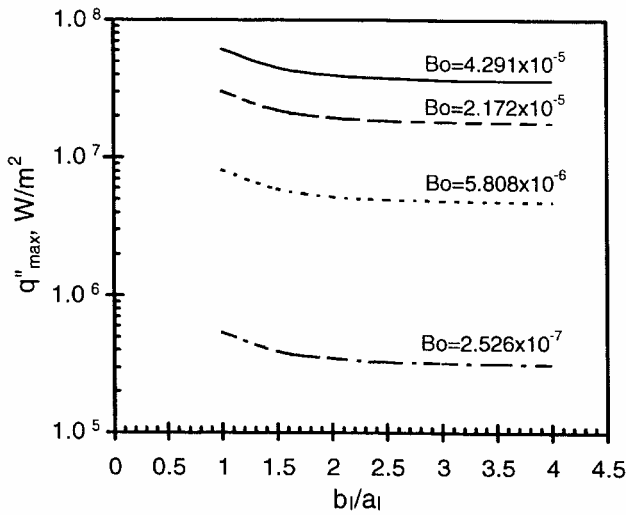


Fig. 6 Geometric effect on the evaporation heat transfer.

where k_{eff} is the effective thermal conductivity of the capillary layer that depends on the physical properties of the capillary structure and the working fluid. It can be specified for different kinds of porous structures.^{5,6}

As indicated, the superheat is proportional to the thickness of the layer. Thinning the liquid film will increase the interfacial evaporation rate caused by a decrease in the thermal resistance. For the same wall heat flux the thinner the porous layer, the smaller the superheat required for interfacial evaporation.

For the two-dimensional fluid flow problem of interest here, the geometric configuration of the porous layer also has a significant effect on the maximum evaporation heat-transfer rate through the changes occurring in the pressure distribution and the frictional pressure drop. The maximum capillary evaporation heat-transfer capacity decreases with increasing the radius of the individual particles, which increase the average pore size, as shown in Fig. 6 for different Bond numbers.

Conclusion

A two-dimensional capillary evaporation model for uniformly heated, thin porous layers has been developed and solved analytically to determine the pressure distribution and from this the maximum capillary evaporation heat flux. Examination of this analytical model indicates that the characteristic properties of the porous structure have a significant effect on both the evaporation heat-transfer performance and the pressure distribution. The structural properties of the porous media can be characterized by the Bond number, and the maximum capillary evaporation heat flux through the thin porous layer increases with increasing Bond numbers. Increasing the thickness of the layer enhances the capillary flow, and the resulting maximum evaporation heat flux is proportional to the thickness of the porous layer. The superheat occurring as a result of the heat transfer through the porous layer also increases proportionally to the thickness of the layer. The maximum capillary evaporation heat flux of the sintered powder layer in the current investigation ranged from 10^5 – 10^8 W/m² and was much higher for the metal mesh screen with water as the working fluid.

Acknowledgments

The authors acknowledge the Office of Naval Research and the National Science Foundation for their support of this work.

References

- Udell, K. S., "Heat Transfer in Porous Media Considering Phase Change and Capillarity—The Heat Pipe Effect," *International Journal of Heat Mass Transfer*, Vol. 28, No. 1, 1985, pp. 77–82.
- Sondergeld, C. H., and Turcotte, D. L., "An Experimental Study of Two-Phase Convection in a Porous Medium with Application to Geological Problems," *Journal of Geophysical Research*, Vol. 82, No. 14, 1977, pp. 2045–2053.
- Tolubinsky, V. I., "Some Peculiarities of Vaporization Process in a Single Cell of the Heat Pipe Wick," *Advances in Heat Pipe Technology*, Pergamon, Oxford, England, U.K., 1982, pp. 375–388.
- Kaviany, M., *Principles of Heat Transfer in Porous Media*, Springer-Verlag, New York, 1995, pp. 617–625.
- Peterson, G. P., *An Introduction to Heat Pipes—Modeling, Testing, and Applications*, Wiley, New York, 1994, pp. 244, 245.
- Faghri, A., *Heat Pipe Science and Technology*, Taylor and Francis, Philadelphia, PA, 1995, pp. 125–245.